Available online at www.sciencedirect.com
ScienceDirect
C. R. Physique 10 (2009) 676–690
COMPTES RENDUS PHYSIQUE

Physics and heritage / Physique et patrimoine

A new high quality X-ray source for Cultural Heritage

Philippe Walter [a,*], Alessandro Variola [b], Fabian Zomer [b], Marie Jaquet [b], Alexandre Loulergue [c]

[a] *Centre de recherche et de restauration des musées de France, CNRS-UMR 171, Palais du Louvre, 14, quai François-Mitterrand, 75001 Paris, France*

[b] *Laboratoire de l'accélérateur linéaire – LAL, Université Paris-Sud 11, CNRS-UMR 8607, bâtiment 200, 91898 Orsay cedex, France*

[c] *Synchrotron SOLEIL, L'Orme des Merisiers Saint-Aubin, BP 48, 91192 Gif-sur-Yvette cedex, France*

Available online 14 October 2009

Abstract

Compton based photon sources have generated much interest since the rapid advance in laser and accelerator technologies has allowed envisaging their utilisation for ultra-compact radiation sources. These should provide X-ray short pulses with a relatively high average flux. Moreover, the univocal dependence between the scattered photon energy and its angle gives the possibility of obtaining a quasi-monochromatic beam with a simple diaphragm system. For the most ambitious projects the expected performance takes into account a rate of 10^{12}–10^{13} photons/s, with an angular divergence of few mrad, an X-ray energy cut-off of few tens of keV and a bandwidth $\Delta E/E \sim 1$–10%. Even if the integrated rate cannot compete with synchrotron radiation sources, the cost and the compactness of these Compton based machines make them attractive for a wide spectrum of applications. We explore here the interest of these systems for Cultural Heritage preservation. ***To cite this article: P. Walter et al., C. R. Physique 10 (2009).***

Résumé

Une nouvelle source de rayons X de haute qualité. Les sources de photons par effet Compton inverse apparaissent aujourd'hui particulièrement prometteuse étant données les avancées technologiques dans le domaine des lasers et des accélérateurs. Il est désormais possible d'envisager leur utilisation en tant que source ultra-compacte de radiations. Elles peuvent fournir des pulses de rayons X très courts avec un flux moyen important. De plus, la relation directe entre l'énergie des rayons X produits dans l'axe de la collision photon–électron permet d'obtenir des faisceaux quasi-monochromatiques avec un simple collimateur. Les projets de telles sources permettent d'envisager des flux de 10^{12}–10^{13} photons/s avec un angle de divergence de quelques milli-radians, une énergie de quelques dizaines de keV et une largeur de bande $\Delta E/E \sim 1$–10%. Si de tels dispositifs ne peuvent pas être considérées comme en compétition avec les installations de rayonnement synchrotron, leur relativement faible coût et leur compacité en font des dispositifs attractifs pour de nombreuses applications. Nous étudions ici leur intérêt dans le domaine de l'étude des matériaux du patrimoine. ***Pour citer cet article : P. Walter et al., C. R. Physique 10 (2009).***

Keywords: X-rays; Chemical analysis; Imaging techniques; Cultural heritage; Inverse Compton source

Mots-clés : Rayons X ; Analyse chimique ; Techniques d'imagerie ; Patrimoine ; Source Compton inverse

* Corresponding author.
E-mail address: philippe.walter@culture.gouv.fr (P. Walter).

1631-0705/$ – see front matter
doi:10.1016/j.crhy.2009.09.001

1. Introduction

Nowadays, cultural heritage plays a crucial role, as far as the quality of life and the attractiveness of France are concerned; it has significant economic effects in many fields. The public at large takes great interest in it, as testified by the high number of visitors flocking to the many French monuments and museums. Consequently, knowing one's cultural heritage and preserving it in order to hand it over to future generations is an increasingly important and shared concern, especially in the European Union. At present in France all levels of society – government, regions, municipalities and private companies – are involved in this effort.

Therefore, the need was felt to carry out fundamental and applied research in order to best preserve this heritage and allow the public to access as many works of art as possible, and learn about their history. On the one hand, in order to make progress in unveiling the history of works of art and archeology it is necessary to identify the materials used; on the other hand, when conserving and restoring artifacts the effects of the aging of the materials cannot be neglected. To this end, the methods commonly used in materials science can prove extremely useful, especially those enabling researchers to perform a non-destructive analysis directly on works of art or on tiny but representative samples.

The characterization of art object materials is a big challenge from an analytical point of view, since there are many materials, they are often available in very small quantities, they have been processed or synthesized and then used by man, they have deteriorated in the natural environment or in the buildings in which they have been kept (museums, libraries, historical monuments, etc.). This is the case for paintings and graphical documents made up of various layers including mineral and organic matter (pigments, colorings, inks, binders, etc.): the chemical interaction between the different elements results in specific changes or deterioration over a very long time. It is therefore necessary to develop and implement a number of innovative techniques to analyze works of arts.

A wide variety of instruments is commonly used. Most of them are classical laboratory techniques, which enable one to probe samples at different levels (atomic, molecular, structural), at different scales (from millimeters to nanometers), and with different sensitivities (major to trace elements). Although lab instruments become more and more powerful and remain the prime equipment for the study of Cultural Heritage objects, two recent evolutions can be underlined. On the one hand, the necessity of reaching sites (excavation sites, museums, monuments, etc.) fostered the development of portable instruments enabling *in situ* analyses. On the other hand, specific studies require a higher level of performance and are only possible on large-scale facilities (ion beam accelerator, synchrotron radiation and neutron sources, electron microscopes) which provide brighter and smaller spots.

For this reason the setting-up of an ion beam particle accelerator in the Louvre premises – labeled AGLAE [1], an acronym for *Accélérateur Grand Louvre d'Analyse Elémentaire* – in late 1988 was a major step in the development of this research work. It made possible to investigate the composition of museum's works of art directly, with the ion beam analysis (IBA) techniques, with a 20–30 μm spatial resolution which was ideal to study very complex and heterogeneous materials [1,2].

The use of ion beam analysis for the study of art works and archaeological artefacts is linked to the development of the particle induced X-ray emission (PIXE) technique in the early 1970s [3]. In this field, information on the elemental composition was previously provided by X-ray fluorescence (XRF) and SEM-EDX, which at that time were only applicable on small samples taken from the objects. The high sensitivity of PIXE, which strengthens the widely recognized non-destructive character of IBA methods, explains its fast growing popularity. Another important fact is the early implementation of PIXE in air [4] which opened the possibility of *in situ* analysis of art objects of large size or too fragile to be put under vacuum. Up to now, AGLAE is the sole facility of its kind to be entirely dedicated to the study of art works and archaeological artifacts. Its use was originally restricted to X-ray and gamma-ray spectroscopies (PIXE and PIGE), first in a vacuum chamber, then with an external millimeter-sized beam [5]. The upgrading given by a focusing system and an ultra-thin exit window enabled:

a) its transformation into a real external nuclear microprobe [6];
b) the implementation in air of other IBA techniques such as Rutherford backscattering spectrometry (RBS), elastic recoil detection analysis (ERDA) and nuclear reaction analysis (NRA) [7].

Today AGLAE is a unique and powerful analytical tool for the characterization of the materials of the museums' works of art. AGLAE is available to foreign researchers in the framework of a EU-financed program. A review of the

Table 1
Requirements table for the analysis techniques used in heritage studies.

	XRF	XRD	XANES	Tomography	Edge enhancement	Phase contrast	Magnification
Energy range [keV]	6.5–92	10–92	6.5–92	20–100	7–100	10–30	10–100
$\Delta E/E$	1–3%	3–10%	5–10%	3% bw	3–10%	3% bw	3% bw
Source size				10–100 μm	10–100 μm	Very small	Very small
Size on the object	20 μm	20 μm	20 μm	10–50 cm	50 cm	50 cm	1–50 mm
Flux on the object [ph/s]	10^9–10^{10}	10^9 ph/s	10^7 ph/s	10^{11}	10^9	10^{11}	10^{11}
Acquisition time	1–60 s	1–300 s	2000 s				
Coherence				No	No	Yes	No

use of accelerators in studies connected to our cultural heritage including medium energy ion accelerators for high energy PIXE is given in [8].

In this framework, the Laboratory of the *Centre de recherche et de restauration des musées de France* (C2RMF-CNRS) aims at developing a new tool for the direct analysis and imaging of works of arts and archaeological items. This will require the co-localization of the present ion accelerator and a very intense X-ray source in a laboratory specialized in "non-invasive" analysis of works of art to be set up in the Louvre security area. These two sources will make it possible to develop additional analysis and imaging methods which would pave the way for the development of a new tridimensional analytical method for studying the museums' works of art to be combined with materials science methods. This will mark a radical change in what we know about masterpieces thanks to much more accurate scientific imaging.

A particular advantage is represented for museum objects as it would be strategically positioned inside the Louvre. There would therefore be no cost constraints and no danger resulting from the need to move the museum's most precious works of art, namely Louvre's paintings, drawings and art objects.

As far as the X-ray production is concerned, in this article, we will explore the interest of an inverse Compton source. Compton X-ray compact sources are extremely interesting for the chemistry component analysis applications and one of the most promising fields is cultural heritage preservation and associated domains. Tuneable and highly monochromatic hard X-rays can be obtained in Compton machines with the use of diaphragms (1–10% bandwidth) or monochromators (0.1% bandwidth). For painting studies, X-ray diffraction, laminography and 3D chemical analysis of pigments should take advantages of such radiation sources.

A great advantage should be acquired by exploiting the complementarities between the analysis worked out by employing ion sources like elastic scattering (RBS, ERDA), the use of nuclear reactions for the detection of light elements, and the hard X-ray techniques. Heavy elements analysis, absorption spectrometry, X-ray diffraction and diffusion, tomography and phase contrast imaging will allow an important widening of the application range in the masterpiece analysis domain. To detect the interesting elements associated to the cultural heritage preservation, by analysis at the absorption edge (XANES), different photon energies are necessary. They correspond to the K edge of most metals and to the Pb and Au L_{III} threshold. This means that a photon energy ranging from 6.5 to 92 keV is necessary. Table 1 illustrates the required radiation performance for the different analysis techniques.

So, by combining ion and photon measurement techniques on the same artwork, it is possible to conclude that a complete material analysis will be worked out. These techniques provide precious information for the dating of the work of art, the techniques employed, and its attribution [9]. An important synergy can be developed in integrated laboratories where physicists, chemists, art critics and historians collaborate in the same framework. Here the compactness of the Compton machine plays a fundamental role. As already said, the possibility to place such a source in an integrated laboratory gives the experts a direct access to the masterpieces from the museum. Indeed, a facility in a remote location would involve extremely important insurance, security and transportation costs.

2. Principles of Thomson and Compton scattering

2.1. Principles and cross section

The diffusion of an electromagnetic plane wave by an electron at rest, with mass m_e and charge q, is a process known as 'Thomson scattering' [10]. From a classical point of view (Fig. 1), the process can be visualised as the diffu-

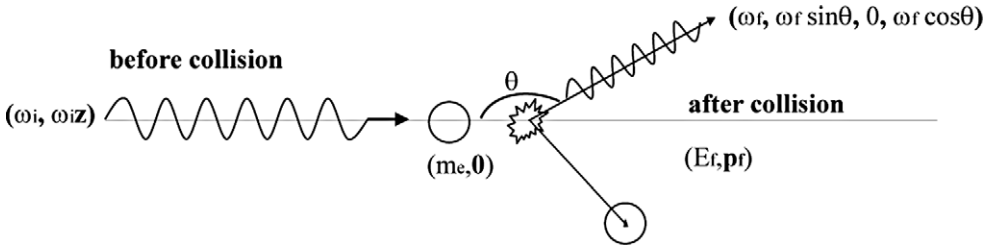

Fig. 1. Two-dimensional representation of the scattering kinematics, in the reference frame where the electron is initially at rest.

sion of a plane wave of frequency ω_i impinging on a charge. The scattered wave is not plane but, in the approximation where the recoil effect can be neglected (therefore taking into account $m_e \gg \omega_i$), its frequency is conserved. On the other hand, in quantum electrodynamics, the scattering process is analyzed as the succession of the absorption and the emission of the photon by the electron.

In the "God-given" units: $c = 1$ and $\hbar = 1$, the differential scattering cross section is:

$$\frac{\mathrm{d}\sigma}{\mathrm{d}\Omega} = \frac{1}{2} r_0^2 \left(1 + \cos^2\theta\right) \tag{1}$$

where $r_0 \sim 2.818 \times 10^{-15}$ m is the classical electron radius and θ is the photon scattering angle with respect to its initial momentum. By integrating over the angular variable, the classical Thomson cross section σ_{Th} is obtained:

$$\sigma_{Th} = \frac{8\pi}{3} r_0^2 = 0.665 \times 10^{-28} \left[\mathrm{m}^2\right] \tag{2}$$

The absolute value of the Thomson cross section can be interpreted as follows: one photon travelling one meter within a target whose density is one electron per one cubic meter has a probability σ_{Th} of being scattered. Depending on the physics application, the scattering probability can be seen as large when compared to typical QED processes, or extremely low as it is the case, for example, in applications which aim at producing very high flux light sources.

The generalisation of Eq. (1), when the recoil of the charged particle cannot be neglected, was given by Klein and Nishina [11]. In this case the kinematics of the process is best described as a collision between the photon and the electron (see Fig. 1) since energy and momentum are conserved. Therefore the scattered photon undergoes a frequency shift. In the reference frame where the electron is initially at rest, the differential Compton cross section is (assuming unpolarised electrons and photons):

$$\frac{\mathrm{d}\sigma}{\mathrm{d}\Omega} = \frac{r_0^2}{2} \left(\frac{\omega_f}{\omega_i}\right)^2 \left(\frac{\omega_i}{\omega_f} + \frac{\omega_f}{\omega_i} - \sin^2\theta\right) \tag{3}$$

where ω_i (i = initial state) and ω_f (f = final state) indicate respectively the photon energy before and after the scattering process. It can be immediately pointed out that, in the limit $\omega_f/\omega_i \to 1$, i.e. in the case where the scattered photon frequency remains unchanged, Eq. (3) takes again the form of Eq. (1).

When considering the collision between a high energy free electron of momentum p_e and a low energy photon, where $p_e \gg \omega_i$, a substantial fraction of the electron energy is transferred to the photon. As a result, in the observer frame, the photon is backscattered with a significant energy boost. This process is known as Compton backscattering, being the relativistic extent of the Compton effect [12].

A simple expression of the total Compton scattering cross section in the center-of-mass frame can be obtained by using the relativistic invariant Mandelstam variables [13]:

$$\sigma_{tot} = \frac{2\pi m e^2 r_0^2}{E_{cm}^2} \mathrm{Log}\left[\frac{E_{cm}^2}{me^2}\right] \tag{4}$$

where E_{cm} is the electron energy in the center-of-mass frame ($E_{cm} = m_e^2 + 2p_f\omega_f(1 - \cos\theta)$).

Nevertheless, from an experimental point of view, the most important results are the differential and the total cross section in the laboratory frame. Neglecting the polarization dependence, the total and differential scattering cross section are:

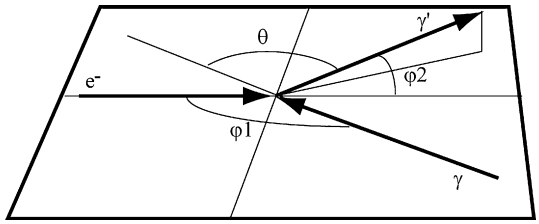

Fig. 2. Scheme of the most general case of a photon–electron collision. The electron incidence angle is φ_1, the photon scattering angle is θ (with respect its initial momentum).

$$\sigma_{tot} = \frac{2\pi r_0^2}{x_1}\left\{\left(1 - \frac{4}{x_1} - \frac{8}{x_1^2}\right)\ln(1+x_1) + \frac{1}{2} + \frac{8}{x_1} - \frac{1}{2(1+x_1)^2}\right\} \tag{5a}$$

$$\frac{\mathrm{d}\sigma}{\mathrm{d}\Omega} = 2r_0^2\left(\frac{\omega_f}{m_e x_1}\right)^2\left(4y(1+y) - \frac{x_1}{x_2} - \frac{x_2}{x_1}\right) \tag{5b}$$

where $x_1 = 2\gamma\frac{\omega_i}{m_e}(1-\beta\cos\varphi_1)$; $x_2 = -2\gamma\frac{\omega_f}{m_e}(1-\beta\cos\varphi_2)$; $y = \frac{1}{x_1} + \frac{1}{x_2}$ where β is the relativistic beta factor and γ is the Lorentz factor equal to $1/(1-\beta^2)^{1/2}$. φ_1 and φ_2 indicate respectively the incidence angle and the scattering angle in respect to the electron direction, as illustrated in Fig. 2. Taking the limit for $x_1 \to 0$ ($\gamma\omega_i \ll m_e$) the second term of the formula Eq. (5a) corresponds within an excellent approximation to σ_{Th} (the limit can be easily solved by expanding in series the function $\ln(1+x_1)$ about zero to the third order). Then the total scattering cross section is very close to the Thomson one.

The spectral density in the ultrarelativistic case is simply obtained starting from (5b) and taking into account the relationship:

$$\frac{\mathrm{d}\sigma}{\mathrm{d}\omega_f} = \frac{\pi m_e x_1}{\gamma\omega_f^2}\frac{\mathrm{d}\sigma}{\mathrm{d}\Omega} \tag{6}$$

The emitted spectrum has a sharp cut-off as far as the backscattered photon energy is concerned. This energy cut-off is proportional to the energy of the impinging photon and varies quadratically with the electron energy. As an example, in Fig. 3 the energy distribution generated by a beam of 1.3 GeV impinging on a 1 eV laser pulse is illustrated. The spectrum cut-off is immediately observable in the distribution histogram, approximately at 30 MeV.

The frequency boost due to the Compton backscattering and the relationship between the scattered photon emission angles and its energy will be discussed in the next paragraph.

2.2. The frequency shift and the emission angular distribution

As previously stated, when the recoil cannot be neglected, the scattered photon undergoes a frequency shift. The scattered photon final frequency is given by:

$$\omega_f = \frac{\omega_i}{1 + \frac{\omega_i}{m_e}(1-\cos\theta)} \tag{7}$$

where one notices that for $m_e \gg \omega_i$ the frequency is conserved after the collision as was previously mentioned.

The specific case of a Compton collision between a free relativistic electron ($p \gg m_e$) and a photon shows very interesting characteristics in the laboratory frame. They originate in the joint effect of the relativistic boost and the Doppler effect. Actually the observer will notice a significant energy boost of the scattered photon and a drastic shrinking of the angular cone of emission. These can also be calculated by using the Mandelstam variables, taking into account the most general collision geometry case of a photon with incidence angle φ_1 [14]. In the laboratory frame the "boosted" frequency shift is:

$$\omega_f = \frac{\omega_i(1-\cos\varphi_1)}{1 - \beta\cos\varphi_2 + \frac{\omega_i}{m_e\gamma}(1-\cos\theta)} \tag{8}$$

that for $\gamma \gg 1 \approx> \frac{2\gamma^2\omega_i(1-\cos\varphi_1)}{1+(\gamma\varphi_2)^2+2\gamma\frac{\omega_i}{m_e}(1-\cos\varphi_1)}$.

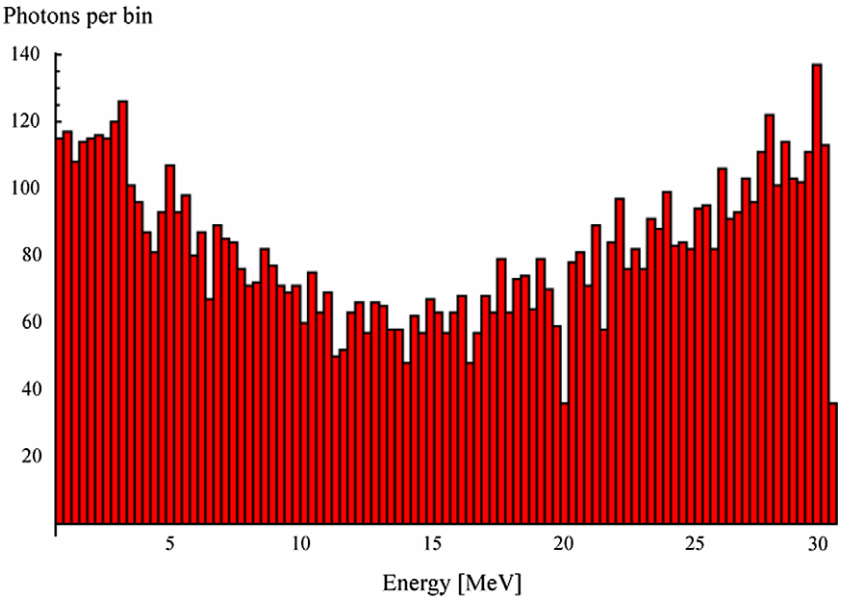

Fig. 3. Compton collision emitted photons energy distribution. The electron beam and laser energies are respectively 1.3 GeV and 1 eV. The energy cut-off is very sharp at ∼30 MeV.

From Eq. (8) it is possible to highlight the dependence of the main properties of the scattered photon on the collision parameters: the photon incidence energy and angle, the electron energy and the photon scattering angle. The Compton back-scattering characteristics are particularly attractive in the relativistic case where they can be summarized as follows:

a) There is a univocal dependence between the scattered photon energy and its angle. This is very effective for selecting the frequencies, and consequently to obtain a monochromatic beam, by setting up a simple diaphragm.
b) The emission cone is shrunk by the relativistic boost. To a good approximation one can assume that the flux is emitted in a solid angle with total aperture $4/\gamma$.
c) The maximum energy boost of the scattered photon occurs in the so-called "head-on" collision ($\varphi_1 = \pi$). In this case the energy spectrum cut-off ω_c, corresponding to the backscattered photon ($\varphi_2 = 0$), varies as $\omega_c = 4\omega_i\gamma^2$. For different collision angles the maximum energy is reduced. If $\varphi_1 = \pi/2$ the scattered photon maximum energy is half the one in the head-on collision case, while the mean direction of the backscattered photons remains close to the electron beam direction.
d) The high value of the scattered photon maximum energy (the energy cut-off) with its quadratic dependence on the electron energy allows the production of high energy X and gamma rays by using a relatively moderate energy electron beam, in the MeV–GeV range.

In Fig. 4, the three-dimensional plot summarizes the dependence of the scattered photon energy on the incidence and scattered angles for different impinging electron energies. One notices that orthogonal collision halves the scattered frequency and that the emitted photon cone shrinks as the energy increases. The different colour curves correspond to different electron energies.

The limit of the angular shrinking is given, in a real experiment, by the fact that the Compton flux is not generated by a single particle but rather by an electron beam with a natural divergence at the interaction point. The resulting angular aperture of the emitted photons will then be given by the convolution between the Compton $1/\gamma$ cone and the electron beam divergence. This is extremely important since, taking into account the angle-energy dependence for the scattered photons, a too strongly divergent electron beam will affect not only the brilliance, but also the possibility to select a monochromatic beam by using diaphragms.

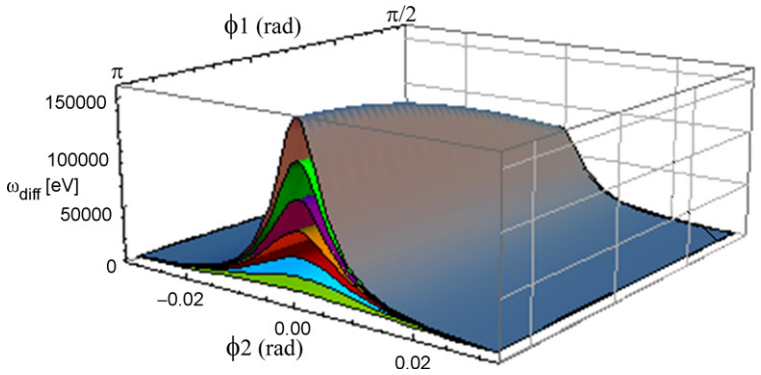

Fig. 4. Scattered photon angle-energy dependence (ω_{diff} vs ϕ_2) for different collision angles ϕ_1. This is varied from the head-on collision ($\phi_1 = \pi$) to the normal incidence ($\phi_1 = \pi/2$). The colour curves represent different electron energies; respectively 100 (brown), 70 (light green), 60 (violet), 50 (orange), 40 (red), 30 (light blue) and 20 MeV (green). The initial photon energy is 1 eV. Calculations worked out with MATHEMATICA®.

2.3. Compton interaction schemes

In a real Compton source, the radiation is generated in a collision between an electron bunch and a laser pulse. This allows increasing the emitted flux by providing interactions between a high number of charged particles and photons. So, first of all, high intensity electron bunches and photon pulses are produced respectively by particle accelerators systems and lasers. At this point there are two different ways to operate a Compton source depending on the envisaged collision repetition frequency f_{rep}:

- If f_{rep} is low (1–100 Hz) an extremely high energy laser pulse is required (0.1–10 J). Therefore a very high instantaneous flux is produced in a single shot. In this case the electron bunch is provided by a Linac delivering a strong charge per pulse. After the collision the bunch is discarded.
- If f_{rep} is high (10–100 MHz) a high average power laser is needed. To increase the laser pulse energy a passive photon pulse stacking can be realised in Fabry–Perot optical resonators. These are composed by high reflectivity mirrors systems. Their basic principle is to continuously stack laser pulses in phase with the circulating injected photons, so that it comes back to the injection mirror by multiple reflections. This results in a linear, "passive" energy amplification of the circulating pulse energy in the cavity. The target is to store in the optical resonator more than 1 mJ per pulse at a very high repetition frequency and to lock its phase with the electron bunch.

In this scheme, after the collision, the electron bunch has to be re-circulated for a successive new collision with the laser pulse stored in the optical resonator. To re-circulate electron bunches, at present, either compact storage rings or Energy Recovery Linac (ERL) are considered. With respect to the first scheme, in this case, there is a net loss of instantaneous flux (photons per collision) but an enormous gain in the number of collisions per second, so in average emitted flux.

Another very important aspect for the flux optimisation is the collision scheme. It is evident that, to increase the interaction probability, it is necessary to strongly focus the two beams in the interaction point (IP) to reduce their transverse cross sections. This will maximize the local interaction density and the results will be that many photons and many electrons will "see each other". However, in the interaction space–time geometry not only the transverse dimensions have an impact. Different parameters are correlated and play a role like the bunch length and the crossing angle.

We can provide two meaningful examples:

1) In the case of head-on collision a limit to the focusing in the collision point is given by the correlation between the transverse bunch dimensions and their lengths. This is known as Hourglass effect.
2) In the case in which a crossing angle is needed the flux will be dependent from the correlation of the crossing angle with the beam lengths. In fact, at constant charge, for longer beams the total overlap time will be reduced due to the interaction angle.

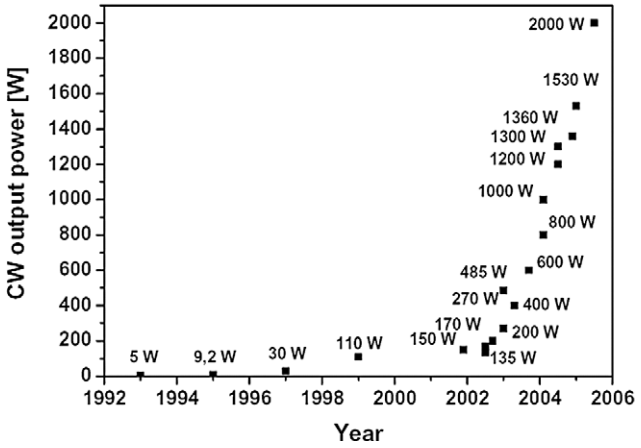

Fig. 5. Power evolution of cw double-clad fiber lasers with diffraction-limited beam quality over the last decade.

Taking into account all these considerations we will be able to define the emitted rate R (photons/s) as $R = L\sigma$, where σ indicates the cross section and L the luminosity. The luminosity is a function that quantifies "how good" is the interaction region design, how intense are the electron and photon beams and how frequent are the collisions. Its dependence on the over mentioned parameters is appreciable in the luminosity analytical expression that takes into account a crossing of two Gaussian bunches, where the Hourglass effect is neglected:

$$L = N_e N_\gamma f \frac{\cos\phi}{2\pi} \frac{1}{\sqrt{\sigma_{ye}^2 + \sigma_{y\gamma}^2}\sqrt{(\sigma_{x\gamma}^2 + \sigma_{xe}^2)\cos^2\phi + (\sigma_{ze}^2 + \sigma_{z\gamma}^2)\sin^2\phi}} \tag{9}$$

where N_e, N_γ, f, ϕ, $\sigma_{x,y,z,e}$, $\sigma_{x,y,z,\gamma}$ indicate respectively the number of electron and photons per bunch, the repetition frequency, the half of the angle of collision and the three-dimensional bunch r.m.s. sizes for the electron (index e) and photon (index γ) bunches. If we want to take into account the Hourglass effect we have to remember that, in case of strong focalization, the transverse dimensions depend by the longitudinal coordinate in the interaction region. The luminosity is a "physics independent" parameter since it takes into account only the collision parameter. The specific rate linked to a particular physics channel can be easily calculated multiplying the luminosity by the cross section.

3. Recent advances in Compton sources

In the last years an impressive progress concerning the laser systems, the optical resonators and the accelerators technology has boosted the proposal of different Compton projects in the world. This concerns hard X-ray and gamma ray photon sources for different applications going from the medical science, the security industry to the cultural heritage.

3.1. Laser amplification

The introduction of new laser amplification technology (fiber lasers, saturable absorber, cryo-cooling, etc.) has increased the pulse and average laser system power by some order of magnitude. One very important example is given by fiber technology that has recently experienced a great expansion. An appropriate illustration of this power "exponential growth" is shown in Fig. 5 where the power attained by the CW fiber laser in the last fifteen years is displayed. One can appreciate the impressive increase after the year 2000.

These new opportunities allowed reaching also in the pulsed regime (the more suitable for Compton sources) average powers of more than 100 W with repetition frequencies that can vary between 70 to 300 MHz. One of the most promising aspects is that the amplification regime seems to be limited only by the pumping power availability (actually diodes are rather expensive), not showing any saturation up to 325 W [15] and 1.1 kW [16] in ps and ns regimes, respectively. In the former case, the pumping efficiency before stretching is 75% below 200 W and slightly

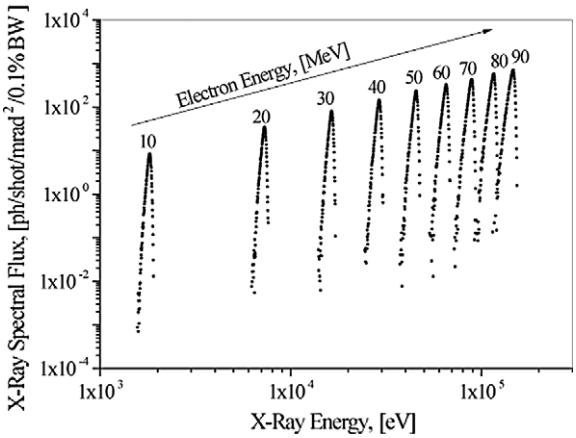

Fig. 6. Calculations of the on-axis X-ray spectra produced by ThomX into 1 mrad^2 for various electron energies.

below 70% above 200 W. This allows one to imagine higher average power fiber laser in the future by adding stacks of diodes.

These power levels, without any further amplification, are not enough to fulfil the Compton source flux requirements. For this reason the laser pulses are stacked in passive Fabry–Perot resonators [17]. To achieve important amplification factors a very good quality laser beam is needed (low phase and amplitude noise, high degree of polarization and robustness, laser beam propagation factor $M^2 \sim 1$. M^2 can be used to parameterize the degree of deviation of the actual beam from the ideal Gaussian one during its propagation). This is now possible thanks to the doped Ytterbium fiber technology [18].

3.2. Optical resonators

Another field that recently has known a great expansion is optical resonator technology. Great advancements in stabilising optical cavities with ps and fs pulses have been obtained in NIST Colorado [17] and MPI Garching [19]. After this, a first Compton utilisation has been performed by Lyncean Technology Inc., a spin-off of the SLAC laboratories [20].

In this field, the CNRS laboratories play an important role. High reflectivity mirrors are produced now routinely by the LMA (Lyon), and the group of LAL (Orsay) has first demonstrated the locking of a low power laser with a gain of 10^4. At present these two groups are involved with the CELIA (CNRS, Bordeaux), in a program (ANR MightyLaser) aiming to lock a 200 W fiber laser to a cavity with a gain bigger than a few thousand. This will allow reaching an absolute world record of 100 kW–1 MW stored in an optical cavity. Taking into account a 100 MHz frequency, this will result in ∼10–30 mJ per circulating pulse (∼10^{17} photons/pulse at 1 μm wavelength).

3.3. Storage ring

At present, one nanocoulomb electron bunch, available at tens of MHz is possible only in the storage ring, where different instabilities act on the circulating beam, increasing its length with a consequent reduction of the luminosity and of the emitted flux. Also in this field important results have been obtained in the last years: the Compton dynamics have been studied and understood. Non-Evaporable Getter (NEG) coatings have introduced a new technology for a drastic pressure reduction in the low energy ring, the vacuum being one of the most important limiting factors for the lifetime in low energy rings. Moreover, electronic feedbacks to control and reduce beam instabilities in the rings have been strongly optimised thanks to the introduction of digital technology.

All these important advancements of the last years have made Compton devices very attractive as compact, monochromatic and relatively low cost X-ray sources. Associated to a 10 mJ laser pulse and 1 nC electron bunch and a 20 MHz storage ring, Compton scattered fluxes can attain the $10^{12}/10^{13}$ level at 50 keV. Fig. 6 shows the X-ray spectra in a cone of 1 mrad^2, calculated for series of electron energies from 10 up to 90 MeV and emitted in a collision.

Table 2
ThomX parameters ranges.

Source explored range	
X energy	6–92 keV
Flux	10^{10}–10^{13} ph/s
Bandwidth	3%
Divergence	<2 mrad
Accelerator	
Ring and injector energies	∼20–70 MeV
Charge	1 nC
Electron bunch length	20 ps r.m.s.
Electron energy spread	0.6% r.m.s.
Non-normalized electron beam emittance	5×10^{-8} π m rad
Electron beam waist sizes	70 μm r.m.s.
Laser	
Intracavity average power	>100 kW
Laser pulse length	1 ps r.m.s.
Laser wavelength	1030 nm
Laser beam focus size	43 μm r.m.s.
Laser pulse energy	30 mJ
Compton f_{rep}	50–200 MHz

3.4. Parameterization of "ThomX" source

Taking into account all these considerations, several French laboratories [21] started to evaluate the feasibility of a compact Compton source: the project ThomX. This was the natural outcome of the different important technological results on Fabry–Perot optical resonators and fiber lasers obtained in these laboratories, and by their strong experience in design and building electron accelerators and storage rings. This allowed, as a first evaluation, to consider a prototype machine with performance at the top of the existing ones. In fact, the goal of the previously mentioned program, financed by ANR, MightyLaser is to allow us to reach a photon pulse average energy in the order of 100 kW–1 MW. This system will be installed in the ATF ring (KEK, Tsukuba, Japan) as a demonstration of an ERL based gamma factory for polarized positron production [22]. The same system integrated in a low energy storage ring allows one to consider a very ambitious program.

In this framework some standard performances were taken into account to provide a machine design, and the parametric dependence of the produced X-ray flux was studied. The main characteristics are summarized in Table 2. Fig. 7 illustrates the basic principle of the ThomX Compton sources. The electrons are produced in an electron gun and subsequently bunched and accelerated in an electron linear accelerator (LINAC). Once they have attained the injection energy they are deflected in the injection line to be stored in the ring. The storage ring is composed of magnetic dipoles that bend the beam, keeping it on the design orbit, and quadrupoles focalizing and confining the beam. The interaction point is between two dipoles where the electron bunch collide with the laser pulse stored in the optical resonator.

As far as the machine is concerned the configuration of a short LINAC injecting in a storage ring was chosen. It is supposed to provide 1 nC electron bunches with a normalized beam emittance of 5 π mm mrad to be injected at 50 Hz in the ring with different energies. To favour flexibility, the ring presents a design based on fold symmetry Double Bend Achromat (DBA): eight dipoles and four straight sections (two long sections of 1.2 m and two short sections of 0.2 m). The focusing of the four arcs is provided by quadrupoles having the advantage to allocate free space in between for sextupoles, correctors, etc. Four set of doublets complete the focusing in the long straight. The ring is composed of 8 dipoles, 24 quadrupoles and 12 sextupoles. The circumference of the ring is 14.57 m providing a revolution frequency of 20.6 MHz. With a 500 MHz RF frequency, the harmonic is 24. The beta functions down to 0.1 m at IP provide an electron beam waist of 70 μm in both vertical and horizontal planes.

For a full parametric study of the Compton source flux performances a single collision event was taken into account, so neglecting the effect of the Compton recoil on the beam dynamics in the multi-recirculation case. This can produce

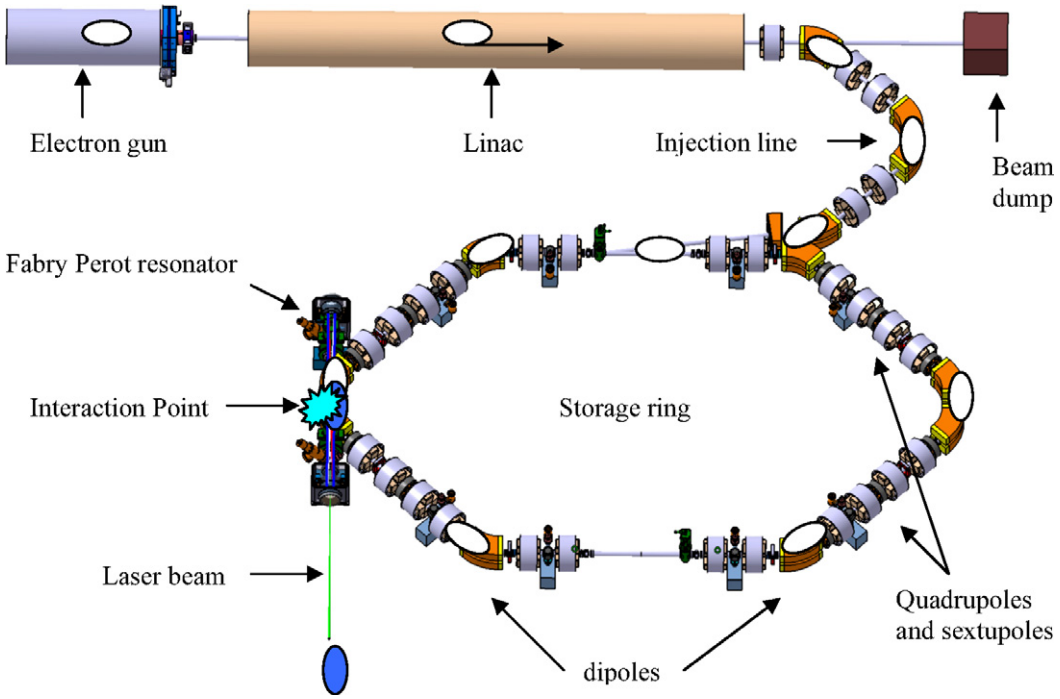

Fig. 7. Scheme of the ThomX X-ray source. The electron bunch is produced in an electron gun, accelerated and injected in the storage ring. Here it is re-circulated colliding with the laser pulse stacked in the Fabry–Perot resonator. The white ellipse illustrates the electron bunch path, the blue one the laser pulse stacking.

a reduction of the total emitted flux in the dynamical regime. The main results obtained have been validated by the comparison with the general analytical luminosity formula (9).

With respect to the previous paragraphs, where an electron–photon collision was considered, the flux emitted in a laser pulse – electron bunch collision presents some fundamental differences. In fact, in a single electron–photon event the photon scattering properties (direction, energy-angle dependence) are mainly dominated by the electron kinematics and the photon diffusion probability. Now, dealing with real bunches, the result will be the convolution between the probability curves and the electron beam divergence in the interaction point. This will imply that:

1) The number of scattered photons per unit angle depends on the electron beam emittance and on the storage ring focalization system.
2) The brightness and the energy angular dependence, so the possibility to obtain a monochromatic beam with a simple diaphragm system, are submitted to the same convolution dependence.
3) Strong laser and electron beam focusing in the interaction point does not correspond to a quadratic increase of the flux due to the Hourglass effect. This takes into account the focalization dependence with respect to the longitudinal coordinate in the interaction region.

One meaningful result is the X-ray spectra in a one mrad^2 cone calculated for different electron energies from 10 up to 90 MeV, illustrated in Fig. 6. The flux per unit angle increases linearly with the electron energy.

To obtain the brightness of the Compton source the maximum spectral value for each peak must be multiplied for the collision repetition frequency (20 MHz) and for the inverse of the square of the electron beam sizes in the interaction point. This allows one to estimate the brightness to $\sim 10^{11}$ ph/s/mm^2/mrad^2/0.1%bw.

It is important to stress that Compton sources are complementary to the third and fourth generation synchrotron radiation facilities since they cannot compete in integrated emitted rates and in brightness. The performances of the most ambitious backscattering sources can be placed near the first generation synchrotron sources but with more attractive characteristics (flux, directivity, monochromaticity, tunability) than other X-ray sources like, for example, X-tubes. Classical bremsstrahlung X-ray tubes can deliver typical spectral rays with a large emission spectrum and

different intensities (rotating anode or microfocus tubes with adaptive optics). At present the rotating anode X-ray tubes associated to a system for X-ray optics, are the most efficient sources if laboratory integration is taken into account. The Rigaku FR-E model with the Vari-max HF optics (Osmic distributed) and a 2.475 kW tube, provide 7×10^9 ph/s maximum flux on a 200 μm diameter surface. Nevertheless these sources do not allow developing more ambitious techniques as far as diffraction, diffusion, absorption, imaging and spectroscopy are concerned. For this reason these latter techniques are commonly used only at the synchrotron radiation facilities.

The ThomX project starts with a pre-defined performance range (Table 1) permitting one to summarize the needs in high average flux, photon energy (tens of keV), bandwidth, divergence, etc. Moreover this prototype will allow acquiring an important experience in operating such a machine and in understanding the subtleties of the beam dynamics under Compton collision regime.

3.5. Development of other projects for various applications

An important feature of Compton sources is the tunability at a specific wavelength obtainable by varying the energy of the electron beam (quadratic dependence) or the wavelength of the impinging laser (linear dependence). This is attractive since a resonant reaction can be triggered by the interaction between the X-rays with a determined energy, and an electronic shell of a contrast agent (like K-shell extraction with a subsequent energy release by Auger cascade). A spin-off of the SLAC laboratory (USA) has created a commercial Compton source [20] for X-ray diffraction of protein, better understanding of disease, more effective drug development, and by enabling clinical applications of emerging new techniques for biological imaging [23,24] where performances close to the synchrotron light source ones are attained. Contrast agents (like gadolinium or platinum) based cancer imaging and therapy could also represent the real breakthrough of the Compton machines in the medical field. The importance of the monochromaticity in biological tissue K-edge interactions is described in [25], where the imaging and therapy applications are illustrated. Pulse length requirements can be very demanding in fast biochemistry studies (hundreds of fs range). Nevertheless, other applications need to be exploited starting from the picosecond range. Other interesting domains can be identified in the fields that usually operate synchrotron radiation sources but that do not need a very high average flux. This is the first example of a working mini-synchrotron based on the Compton effect. Moreover, due to the quadratic dependence of the Compton energy cut-off on the electron beam energy, it is easy to imagine harder photon production. This allows one to envisage different applications in the nuclear waste management and treatment industry [26] and in the field of nuclear isotope detection applied to infrastructure security [27].

4. Scientific impact in Cultural Heritage studies

4.1. Analytical methods

Nowadays, the main research activities carried out in the laboratories working in the Cultural Heritage field focus on the identification of materials from a chemical and structural point of view (mineral, organic, hybrid, condense matter), the study of processes used for the elaboration of the works of art (origin of the materials, recipes of chemical synthesis, metallurgy, mechanical treatments and thermal annealing) and the study of alteration and aging behavior, including the issues concerning the preventive conservation and the restoration. The ancient materials may be of natural origin, such as the gemstones, or stem from an artificial preparation at high temperature (glasses, ceramics and metals), or by wet chemistry, for the synthesis of pigments or pharmaceuticals for instance. Other materials have plant or animal origins, such as residues found in vases, sculptures made of wax, and human remains. Sometimes, it is the understanding of a diffusion mechanism, the observation of a patina on metals or the nature of nanocrystallized inclusions which are the purpose of the researches.

These activities require developing specific and appropriate physico-chemical analytical methods for the study of the cultural heritage masterpieces. More than a dozen techniques may be involved as far as painting is concerned [28]. It is possible to highlight the importance of applying a combination of different techniques to detect the underlying nature of the materials employed by the artists. Another important aspect of differentiation is that whereas in certain techniques a sample must be taken, the others allow for an *in situ* analysis of the objects of art [28].

The integration of a high flux monochromatic X-ray source, complementary to AGLAE, will provide a unique opportunity to have at one's disposal methods for non-invasive elementary and structural analysis. A 20 μm resolution,

similar to that currently attained in AGLAE, is particularly well suited for the non-invasive study of ancient materials that often represent complex and heterogeneous samples.

Such an instrument should solve many problems in the context of different scientific cases. The ion beams are unique for the detection of light elements and the measurement of concentration gradients by nuclear reactions and also by elastic scattering (RBS and ERDA). Hard X-rays offer the opportunity to analyze heavy elements with high accuracy, to explore their environment by absorption spectrometry and to better understand the material organization by X-ray diffraction or small angle X-ray scattering (SAXS). By combining these two measurement categories on the same object, it is possible to assume that a "*total analysis of the material*" will be worked out. This will remove all the ambiguity in the interpretation of their nature in all the possible cases, independently from the crystalline or amorphous nature of the sample, from metals to natural compounds.

4.2. X-ray imaging based on different physical properties

The use of radiography for the study of museum masterpieces has developed very rapidly after the discovery of X-rays by Röntgen in 1895. Today, C2RMF has 5 conventional radiography devices on the Louvre site. In the case of paintings, radiography provides information on the artist's techniques, the primitive draft variations, the paint overlays, and the conservation of the work. It reveals, for example, cracks in the paint layer. However, the interpretation of a work of art is much more than a merely conservation status analysis; it falls into the depths of the personality of the artist and sometimes shows the path of an artist toward his work of creation. Radiography is very important to characterize objects, in particular in view of their restoration and to better understand the internal structure, i.e. the inhomogeneities (earth, plaster, bronze, inclusions, and bubbles), the formatting procedures (hammering, casting, lost wax or reversed, etc.), the assemblies, the alterations and the restorations.

An X-ray monochromatic intense source offers the opportunity to develop new techniques for three-dimensional imaging analysis of works of art aiming to a "*perfection level in direct imaging techniques*": combining other imaging techniques in the visible, UV and near IR ranges, it will allow providing a new scientific imaging report on each studied artefact, from the surface to the heart of the matter, with a spatial resolution of recording up to the micrometer scale. These scientific records will complement the documentation about the provenance and the historical and cultural environment of work of art and archaeological objects.

The possibility of using a point source, monochromatic and coherent X-ray beam makes it possible to consider different approaches:

(1) *Absorption tomography*: This technique, commonly used in medicine, shows a fast development in recent years. However, to access to high quality of reconstruction and to quantitative data, an excellent signal to noise ratio is essential. It allows rapid data acquisition at very high spatial resolutions, resulting in precise mapping of the internal structures of the artefact. The use of an intense monochromatic beam is also preferable to conventional X-ray tubes because it avoids beam hardening effects that are frequently strong. This technique is hardly used when dealing with objects almost flat, such as paintings: in this case the X-ray laminography technique should be used.

(2) *Distribution of specific chemical elements analysis*: The edge-enhancement imaging technique is based on the same principle as the angiography of blood vessels in medicine. It is considered that each chemical element, with enough quantity in the work of art, may serve as a contrast agent when imaging with different X-ray energies. In medicine, ions are usually injected in the vascular system. On the other side, as far as the paintings are concerned, lead, tin and mercury are characteristic of the different employed pigments. Therefore these images will map the spatial distribution of the chemical element. In practice, two images on each side of the K (or L) atomic absorption edge are measured. This technique and the resulting quantitative measurements can provide new information on the artist painting methodology: the substructure of a painting provides insight into the genesis of the object. Underlying layers may include the underdrawing, underpainting and modifications to the original sketch. In a growing number of cases conservators have discovered abandoned compositions on paintings, illustrating the artists' practice to re-use a canvas or panel and paint new compositions on top of existing ones. A painting from Vincent Van Gogh has been recently revealed by synchrotron-based XRF mapping [29].

(3) *The phase contrast*: An inverse Compton scattering source should allow developing techniques of phase contrast imaging. These present the important advantage of the contrast enhancement in the case of low density materials.

This is possible since the acquired image records the phase variations of the electromagnetic wave that occur when a variation of the refractive index occurs. The interest of this technique has been demonstrated on fossils in paleontology and on amber samples [30].

(4) *Magnification*: When the X-ray source sizes are very small and the emitted radiation sufficiently divergent (conical beam), it is possible to obtain a geometric magnification factor of the image by moving the detector away from the object. Thus, the projection of the object image is magnified, allowing a better accuracy in detecting details.

Other approaches could also be useful (Diffraction enhanced imaging, holo-tomography, X-ray grating interferometry, etc.).

5. Conclusion

The main appeal of the Compton sources is to provide a high quality X-ray beam from a source that can be easily hosted in a limited area, for example in a university laboratory, a hospital, a museum. The price is consequently strongly reduced with respect to the synchrotron sources.

The installation of a new X-ray source in the Louvre museum, simultaneously coupled with visible imagery and ion beam analysis, will provide useful data for the study of the paintings and the archaeological objects (Table 1). Obtaining images of the surface and the core of the work of art, with spatial resolutions of the order of micrometers, is expected to provide to the researchers the access to digital reconstructions, with a much easier access than the original works. This will avoid endangering the conservation of museum pieces which are particularly fragile: human remains and bones, wood or ivory masterpieces of the prehistoric era from the Musée de l'Homme, the National Museum of Prehistory and the National Archaeological Museum, the objects of ancient or medieval art from the Louvre Museum and the National Museum of the Middle Ages, etc.

Acknowledgements

The authors are grateful to Nikolay Artemiev for calculations of the expected flux. The study of the potential applications of new X-ray sources for Cultural Heritage science was supported by the Eu-Artech European program. The development of the lasers and Fabry–Perot cavity is supported by the MightyLaser program from the ANR.

References

[1] J. Salomon, J.C. Dran, T. Guillou, B. Moignard, L. Pichon, P. Walter, F. Mathis, Nucl. Instrum. Methods B 266 (2008) 2273–2278.
[2] G. Amsel, M. Menu, J. Moulin, J. Salomon, Nucl. Instrum. Methods B 45 (1990) 610.
[3] G.M. Gordon, H.W. Kraner, J. Radioanal. Chem. 12 (1972) 181.
[4] G. Deconninck, J. Radioanal. Chem. 12 (1972) 157.
[5] T. Calligaro, J.-C. Dran, H. Hamon, B. Moignard, J. Salomon, Nucl. Instrum. Methods B 136–138 (1998) 339.
[6] J.C. Dran, J. Salomon, T. Calligaro, Ph. Walter, Nucl. Instrum. Methods B 219–220 (2004) 7–15.
[7] T. Calligaro, J.-C. Dran, E. Ioannidou, B. Moignard, L. Pichon, J. Salomon, Nucl. Instrum. Methods B 161–163 (2000) 328.
[8] H.E. Mahnke, A. Denker, J. Salomon, Accelerators and x-rays in cultural heritage investigations, C. R. Physique 10 (7) (2009) 660–675, this issue.
[9] M. Cotte, E. Welcomme, V.A. Sole, M. Salome, M. Menu, Ph. Walter, J. Susini, Anal. Chem. 79 (2007) 6988–6994.
[10] J.D. Jackson, Classical Electrodynamics, third edition, John Wiley and Sons, 1999.
[11] O. Klein, Y. Nishina, Z. Phys. 52 (1929) 853 and 869.
[12] A.H. Compton, Phys. Rev. 21 (1923) 715.
[13] M.E. Peskin, D.V. Schroeder, An Introduction to Quantum Field Theory, The Advanced Book Program, 1995.
[14] P. Rullhusen, X. Artru, P. Dhez, Novel Radiation Sources using Relativistic Electrons, Series on Synchrotron Radiation Techniques and Applications, vol. 4, World Scientific, 1998.
[15] T. Eidam, et al., Advanced Solid-State Photonics, OSA Technical Digest Series, Optical Society of America, 2009, paper MD3.
[16] O. Schmidt, C. Wirth, I. Tsybin, T. Schreiber, R. Eberhardt, J. Limpert, A. Tünnermann, Opt. Lett. 34 (2009) 1567–1569.
[17] J.R. Jones, J.-C. Diels, J. Jasapara, W. Rudolph, Opt. Commun. 175 (2000) 409–418.
[18] J. Boullet, Y. Zaouter, R. Desmarchelier, M. Cazaux, F. Salin, E. Cormier, Opt. Express 16 (2008) 17891.
[19] C. Gohle, T. Udel, M. Herrmann, J. Rauschenberger, R. Holzwarth, H.A. Schuessler, F. Krausz, T.W. Hänsch, Nature 436 (2005) 234.
[20] http://www.lynceantech.com/.
[21] http://sera.lal.in2p3.fr/thomx/.

[22] A. Variola, C. Bruni, O. Dadoun, R. Chehab, M. Kuriki, T. Omori, J. Urakawa, L. Rinolfi, A. Vivoli, F. Zimmermann, Particle Accelerator Conference (PAC09), Vancouver, Canada, 2009.
[23] M. Ando, C. Uyama, Medical Application of Synchrotron Radiation, Springer-Verlag, 1998.
[24] P. Suortti, W. Thomlinson, Phys. Med. Biol. 48 (2003) R1.
[25] G. Margaritondo, Y. Hwu, J.H. Je, Rivista Nuovo Cimento 27 (2004) 1.
[26] R. Hajima, T. Hayakawa, N. Kikuzawa, E. Minehara, J. Nucl. Sci. Technol. 45 (5) (2008) 441–451.
[27] C.P.J. Barthy, F.V. Hartemann, UCRL-TR 206825, LLNL laboratory report.
[28] M. Cotte, J. Susini, V.A. Solé, Y. Taniguchi, J. Chillida, E. Checroun, P. Walter, J. Anal. At. Spectrom. 23 (2008) 820–828.
[29] J. Dik, K. Janssens, G. Van Der Snickt, L. van der Loeff, K. Rickers, M. Cotte, Anal. Chem. 80 (2008) 6436–6442.
[30] P. Tafforeau, R. Boistel, E. Boller, A. Bravin, M. Brunet, Y. Chaimanee, P. Clotens, M. Feist, J. Hoszowska, J.J. Jaeger, R.F. Kay, V. Lazzari, L. Marivaux, A. Nel, C. Nemoz, X. Thibault, P. Vignaud, S. Zabler, Appl. Phys. A 83 (2006) 195–202.